The Thesis Committee for Kevin Chen
Certifies that this is the approved version of the following thesis:

Gear Ratio Optimization of One- and Two- Speed Transmissions for Fully- Electric Vehicles

APPROVED BY
SUPERVISING COMMITTEE:

Supervisor:

Dongmei Chen

Raul G. Longoria

Gear Ratio Optimization of One- and Two-Speed Transmissions for Fully-Electric Vehicles

by

Kevin Chen, B.S.M.E.

Thesis

Presented to the Faculty of the Graduate School of

The University of Texas at Austin

in Partial Fulfillment

of the Requirements

for the Degree of

Master of Science in Engineering

The University of Texas at Austin

May 2017

Acknowledgements

I would like to thank Dr. Chen for reviving my interest in system modeling and robotic controls in her dynamic systems and controls course. Without her support, advice, and inspiration, I would not have continued down this career path to the completion of this thesis and on to my upcoming career in robotics engineering.

I would like to thank Dr. Longoria for contributing his time as a member of my supervising committee. Without his support in my endeavors, I am certain that my graduate studies would not have been as memorable of an experience, especially in helping me complete my application to participate in a research program in Germany.

We would like to thank Liaoning Shuguang Automotive Group Co. Ltd. for sponsoring this research and providing project specifications.

I would like to thank Terrie Chandler for her logistical support in completing my studies. Without her planning and advice, I would not be finishing my studies so soon.

I would like to thank my parents for supporting me in completing my graduate education and urging me to finish when I was prepared to quit and go into industry instead.

I would like to thank my girlfriend for putting up with the late nights, absent days, and stress of completing my graduate studies and for supporting me through it all.

I would like to thank my old high school robotics team, FRC Team 118 – The Robonauts – for lighting the spark that got me started on a career path as a robotics engineer. I would not be where I am today without you.

Abstract

Gear Ratio Optimization of One- and Two- Speed Transmissions for Fully-Electric Vehicles

Kevin Chen, M.S.E.

The University of Texas at Austin, 2017

Supervisor: Dongmei Chen

Currently, electric vehicles use a transmission with a single-speed fixed gear ratio optimized for performance. This work features the development of a framework to optimize the gear ratio for a given vehicle design, motor efficiency map, motor noise spectrum, and transmission noise spectrum. The framework provides a methodology for designing the optimization problem to be solved using derivative-free optimization methods.

As electric vehicles become increasingly prevalent in the global automotive market, the need to develop multi-speed transmissions to provide a competitive edge against other electric vehicles. This work also explores the optimization of gear ratios for a two-speed transmission and identifies a corresponding switching point to switch between the two ratios. Using the same methodology, the optimization problem is formatted such that derivative-free optimization methods can be used to solve the optimization problem quickly and efficiently.

Utilizing the framework developed, the program was able to identify an optimal gear ratio for a single-speed transmission in about half the time it took a brute-force search method to the same. The two-speed optimization process completed about 50 times faster than the brute force search. In both cases, the result returned by the optimization process was compared against the brute force search result to confirm global optimality. The single-speed gear ratio optimization, the two-speed gear ratio optimization, and the two-speed switching point optimization reliably located a global optimum.

Table of Contents

List of Tables

List of Figures

1 Introduction

1.1 Project Definition

In January 2016, a project involving the optimization of a transmission for the maximization of motor and transmission efficiency and the minimization of motor and transmission noise was proposed. In particular, a transmission design that would show an improvement in efficiency by at least three percentage points and a decrease in sound pressure levels of at least three decibels against a preexisting design was requested.

A Powerpoint detailing preexisting design specifications was included in the original proposal. The parameters provided in the specifications are shown in Appendix A. Beyond the information in Appendix A, no further information had been provided and the development of this project was left open-ended. The project team decided to focus on optimizing the gear ratio of an electric vehicle transmission to maximize efficiency and minimize acoustic noise with the potential for future work in the development of a full transmission and accompanying finite element model to more accurately reflect performance characteristics.

1.2 Thesis Outline

Chapter 2 details the information found in research when developing this software and provides several justifications for pursuing such a project. Chapter 3 provides detailed examples of the data used in this project and the equations used to apply the data to the project. Chapter 4 explains the optimization method used to determine optimal gear ratios and switching points and the framework developed to execute the optimization method. Chapter 5 presents the results of this project, validates the optimization results against results obtained from a global search, and provides a discussion on the findings. Chapter 6 summarizes the results of this project, its contributions, and future work recommendaitons.

2 State of the Art

2.1 System Models

2.1.1 Drive Cycle Models

The National Renewable Energy Laboratory (NREL), has developed an ADvanced VehIcle SImulaOR (ADVISOR) to model performance of vehicles over a set of 40 drive cycles, including those used by the United States and the European Union for emissions testing [1]. These drive cycles provide data on velocity demands over time. Acceleration, force, and torque requirements for the vehicle can be derived from these data points. A more in-depth discussion on the contents of the drive cycle database and their implementation in this project is given in Section 3.2.

2.1.2 Motor Models

2.1.2.1 Motor Efficiency Models

Electric motors have become increasing popular in automotive applications due to the immediate availability of DC power in cars, their high operational efficiencies, and high stall torques [2]. These motors can operate with 85 to 95 percent efficiency and at low speeds, provide very high accelerations that make them ideal for urban vehicles that regularly experience stop-and-go traffic [2]. Developing an accurate model for motor performance requires an intimate knowledge of the construction of the motor and its features such as stator pole design and input current frequencies [2].

These parameters have not been provided and are not immediately available, which made it difficult to develop accurate models of motor performance. Instead, the overall efficiency performance of electric motors is published in the form of torque-speed efficiency maps, which are easily obtained, especially when shopping for electric motors.

An example electric motor efficiency map and its implementation in this project are given in Section 3.4.

2.1.2.2 Motor Acoustic Models

In the past, electric motors have not played a prominent role in areas where noise has been a major concern. However, with the emerging market for electric vehicles, the acoustic performance of electric motors has become increasingly important and requires detailed analysis for high-frequency noise minimization [3]. Currently, numerical analysis methods for electric motor optimization feature the use of a three-component model: an electromagnetic model, a mechanical model, and an acoustic model [3][4]. These models are typically developed independently to accurately model each subdomain and are only useful when they are computationally cheap [3]. Finite element models (FEM) are the primary models with which these systems are analyzed [3][4][5][6]. These models, however, are very computationally expensive and require hours of computation time and design iterations to complete [3].

Studies of electric motor noise have demonstrated that while electric motor noise is not loud, they tend to be at higher frequencies, which has a higher annoyance factor and reduces the sound quality of the vehicle [3]. Once a FEM has been developed for an electric motor, its acoustic performance is output in the form of an acoustic spectrum to be used to assess and mitigate the production of these high-frequency sounds [5][7]. An example acoustic spectrum is shown and explained in greater detail in Section 3.5.

Based on the outputs of these analytical models, there have been attempts to identify critical sources of noise and to reduce their effect on overall acoustic performance. While there are many contributing factors, Islam and Husain have identified unbalanced radial magnetic forces as the primary source of acoustic noise [6].

Modeling and computing the effects of these forces is both computationally expensive and impossible without intimate knowledge of the motor design, which is proprietary and has not been provided. As such, motor acoustic spectra are used as a black-box model for assessing motor acoustic performance in this project.

2.1.3 Transmission Models

Like for electric motors, studies on the acoustic performance of transmissions have increased in recent years, especially due to the fact that electric motors do not produce the low-frequency masking sounds that internal combustion engines do [8]. As in the case of electric motors, there are numerous sources of acoustic noise in transmissions and the primary factors leading to a passenger's ability to hear transmission whine are vibrations at the source, the path through which the noise transmits, and other noises that can mask transmission whine [9].

Vibrations at the source typically come as a result of poor gear meshing [9] and several attempts have been made to address the problem at the source [10]. However, since the internal components of a transmission are tightly packed to reduce volume, internal noise mitigation is limited by the ability to optimize gear geometry in a small space [10][11]. Thus, there have been attempts to develop enclosures to attenuate the noise produced by the gears [10], but even with these enclosures, transmissions may still be noisy once installed in a full system even if quiet on a development test bench [8][9].

To attempt to catch design flaws that lead to loud transmission performance, there have been several attempts to develop models that anticipate transmission acoustic performance [11][12]. These models use either boundary element models (BEM) or finite element models (FEM) to analytically determine acoustic performance [11][12]. However, these models are also computationally expensive, requiring hours of computation time to

determine performance at various frequencies [11]. As a result, there have been attempts to reduce the degrees of freedom to be computed and the development of other more efficient models to reduce computation time [11][12].

The development of these models, like for electric motors, requires intimate knowledge of the transmission's design, which has not been provided and is not publicly available. An undisclosed source has graciously provided proprietary experimental acoustic data for a commercial transmission. Further details are provided in Section 3.6.

2.2 Optimization Methods

2.2.1 Derivative-Free Optimization

Historically, optimization methods have required the ability to compute gradients and Hessians of the objective function. It was not until 1961 that the first derivative-free optimization algorithm – the Hooke and Jeeves algorithm – was developed, due to the computational effort required to solve problems with computationally expensive objectives [13]. Since then, with increasing computational power, research into derivative-free optimization has very gradually increased. Though, due to their inefficiency compared to gradient-based methods, they still have not played a prominent role in academic research. In fact, the first textbook on derivative-free optimization methods was not published until 2009 [14].

One of the most prominent methods of derivative-free optimization is the Nelder-Mead simplex method, which despite being developed in 1965, continues to be used as an effective means of solving optimization problems where the gradient is not available [15]. Several more recent works have continued to improve the Nelder-Mead simplex method for greater efficiency and the formulation developed by Lagarias et al. is implemented in

MATLAB's fminsearch function [16]. A more in-depth explanation of how the Nelder-Mead algorithm works is provided in Section 4.1.

Several other derivative-free optimization methods have been developed both for local searches and global searches. In determining local optima, generalized pattern searches and set searches have been developed, which poll different search directions about a point to determine a direction of descent [16]. Local model-based methods have been developed that seek to develop a model to approximate or bound performance of an objective function in a given region such that the model is easily solved using existing gradient-based methods [16].

For global searches, the methods developed feature an expansion or parallel implementation of local optimization methods. Deterministic methods feature searches based on partitioning the objective function into increasingly small search spaces until a global optimum is found [16]. Global searches also feature model-based searches, which like local model-based searches, attempt to approximate or bound the objective function with a model that is easily solved with gradient-based methods [16]. Global search methods also feature stochastic search methods that may not always move in a direction of descent, but will move in a direction of descent on average [16].

A study of 17 commercially-available implementations of derivative-free optimization methods has been conducted by Rios and Sahinidis [16]. They attempted to demonstrate the ability of each optimization algorithm to find the globally optimal solution for a given set of problems and to assess if there existed a minimum cardinality of solvers that would guarantee success. The study showed that no one solver was capable of guaranteeing success in identifying a globally optimal point, even in the case where the objective functions were convex and smooth [16]. In the case of nonconvex, nonsmooth objectives, such as the one implemented in this paper, no one solver or set of solvers was

capable of guaranteeing convergence to the global minimum [16]. For this project, fminsearch was selected as the commercial solver to use due to its ease of use and existing MATLAB implementation.

2.2.2 Transmission Optimization

While there have been attempts to optimize the design of individual components of an electric powertrain [11], the background research conducted showed little research conducted in the development of transmission optimization methods for electric vehicles. There have, however, been numerous papers published on the subject of transmission optimization for internal combustion engine vehicles and hybrid-electric vehicles.

Of the electric vehicle transmission optimization papers found, one utilized dynamic programming to determine two gear ratios and a switching schedule that would provide the lowest change in state of charge [19]. The other provided a comparison between a single-speed transmission, a two-speed transmission, and a continuously variable transmission for electric vehicles in terms of energy consumption [20].

Our research has not shown the inclusion of motor or transmission whine in the development of these optimization formulations. As a major focus this project is not only optimizing performance of the vehicle, but also in the reduction of acoustic noise, this project formulation still provides a valuable contribution to the area of electric vehicle transmission design.

2.3 AIM OF THIS WORK

Based on the project demands and the information provided to the project team, the focus of this project was the development of a framework with which gear ratio optimization for a drive cycle set, motor, and transmission can be done not only to maximize performance, but also to minimize noise. As has been noted in the research into

the state of the art, accurate models for the motor and transmission require a fully fleshed-out design and an accompanying FEA model. Since neither has been provided and both require design work that was determined to be beyond the scope of this project, the framework utilizes a black-box model for the motor and transmission to extract critical information with the assumption that more accurate models can be developed in the future to improve optimization results. The remainder of this thesis seeks to justify the design choices behind the system modeling and methodology pursued to create this framework.

3 System Model

3.1 VEHICLE CHARACTERISTICS

At the most basic level, optimizing vehicle performance requires vehicle parameters to model vehicle dynamics. This project modeled both a loaded and an unloaded vehicle for analysis. The vehicle models contained the following parameters: frontal area, aerodynamic drag coefficient, tire friction coefficients, tire radius, vehicle mass, and rear axle load. The specific values are detailed in Appendix B.

3.2 DRIVE CYCLES

3.2.1 Drive Cycle Data

To obtain vehicle performance demands, the automotive industry uses a series of drive cycles – some proprietary, some publicly available – to determine the efficiency of motor vehicles. Each drive cycle provides vehicle demands over a set course as velocity demands over time. A sample drive cycle is shown in Figure 3.1.

One commonly used software package for vehicle analysis is NREL's ADVISOR, which simulates vehicle performance over a collection of 40 drive cycles. These 40 cycles were extracted from the ADVISOR software for use in gear ratio optimization to provide a wide variety of scenarios in which the proposed electric vehicle may be used. A full list of the 40 drive cycles can be found in Appendix C.

3.2.2 Drive Cycle Preparation

To compute the motor and transmission demands for each drive cycle, the drive cycle demands needed to be converted from linear speed demands to rotational speed demands:

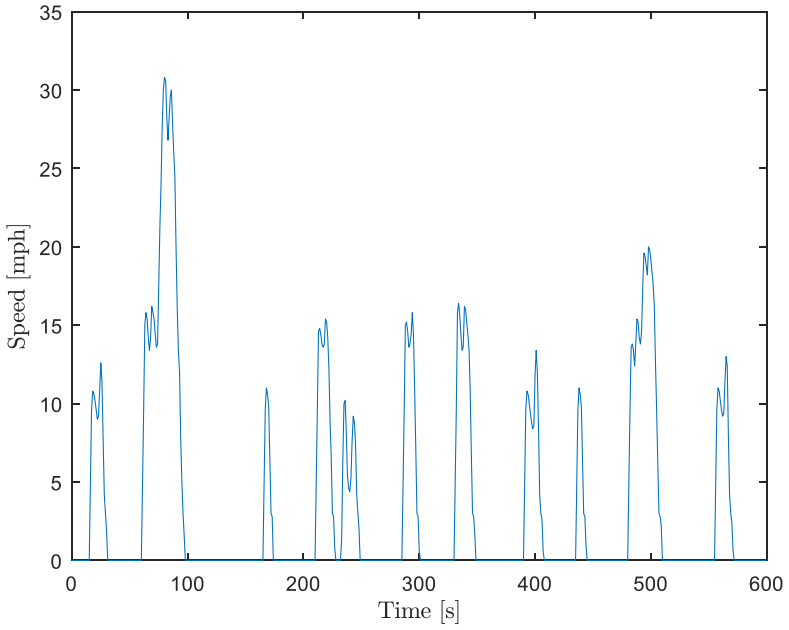

Figure 3.1: New York City bus drive cycle

$$\omega_t(t) = \frac{V(t)}{R} \tag{3.1}$$

Torque requirements at each time point also needed to be precomputed to provide an efficient computation of vehicle performance. The torque output required from the transmission is given as follows:

$$\tau_t(t) = \tau_a(t) + \tau_d(t) + \tau_f(t) \tag{3.2}$$

To compute the torque required to accelerate the vehicle, τ_a, a discrete-time computation of acceleration based on drive cycle demands first needed to be conducted:

$$a(t) = \frac{V(t) - V(t + \Delta t)}{\Delta t} \tag{3.3}$$

From this information, the acceleration torque requirement could be computed:

$$\tau_a(t) = MRa(t) \tag{3.4}$$

The torque required to overcome aerodynamic drag and rolling friction could be computed by Equations 3.5 and 3.6, respectively:

$$\tau_d(t) = \frac{1}{2} C_d \rho A R [V(t)]^2 \tag{3.5}$$

$$\tau_f(t) = \mu_r M g R \tag{3.6}$$

An important thing to note is that the discrete-time computation of acceleration demands yielded one fewer data point than was provided for velocity demands. As such, $a(0)$ was assumed to be zero. Additionally, since the drive cycle analysis looked specifically at the case where the motor is in use, non-positive accelerations points were set to zero, since they would be handled by brakes, rather than the motor, assuming that regenerative braking is not implemented.

For rolling friction, $\tau_f(t)$ was given a value of zero for points that have a non-positive velocity, since rolling friction would not contribute to the vehicle dynamics in a meaningful manner unless the vehicle is moving forward.

Finally, in early implementations of the optimization software, the non-smooth characteristics of some drive cycles extracted from ADVISOR caused the energy requirement computation to fail by causing large, discontinuous spikes in acceleration

demand. As such, a moving-window averaging method was used to smooth out the drive cycles before computing the aforementioned rotational velocity and torque requirements:

$$V(t) = \frac{1}{2N} \sum_{k=-N}^{N} V(t + k\Delta t) \tag{3.7}$$

Combining all of these equations yielded a smooth dataset of rotational velocity and torque points over a given drive cycle for vehicle performance simulation. All of the data were stored in a matrix detailing time points, t, transmission output velocity demand, $\omega_t(t)$, and transmission output torque demand, $\tau_t(t)$.

3.2.3 Drive Cycle Energy Requirement

Given vectors for transmission output torque and transmission output speed requirements, $\vec{\tau}_t$ and $\vec{\omega}_t$, respectively, and a constant time step, Δt, the required energy output at the transmission output was given by the following equation:

$$E_t = \langle \vec{\tau}_t, \vec{\omega}_t \rangle \Delta t \tag{3.8}$$

3.3 Transmission Dynamics Model

Based on the research conducted for this project, it was determined that an advanced transmission model could not be constructed without a completed design with FEA analysis. As such, the transmission model used in this program was assumed to be 100% efficient and only affects system performance by changing the motor speed and torque demands. The motor speed and torque demands could be computed using the linear relationship between the input and output of a transmission:

$$\tau_m(t) = \frac{\tau_t(t)}{r} \tag{3.9}$$

$$\omega_m(t) = r\omega_t(t) \tag{3.10}$$

3.4 MOTOR EFFICIENCY MODEL

3.4.1 Motor Efficiency Data

Electric motor performance is typically provided in the form of a torque-speed curve. These curves detail the maximum achievable torque at a given rotational output speed for the motor as well as the efficiency at a given operating point. Such a torque-speed efficiency map is shown in Figure 3.2.

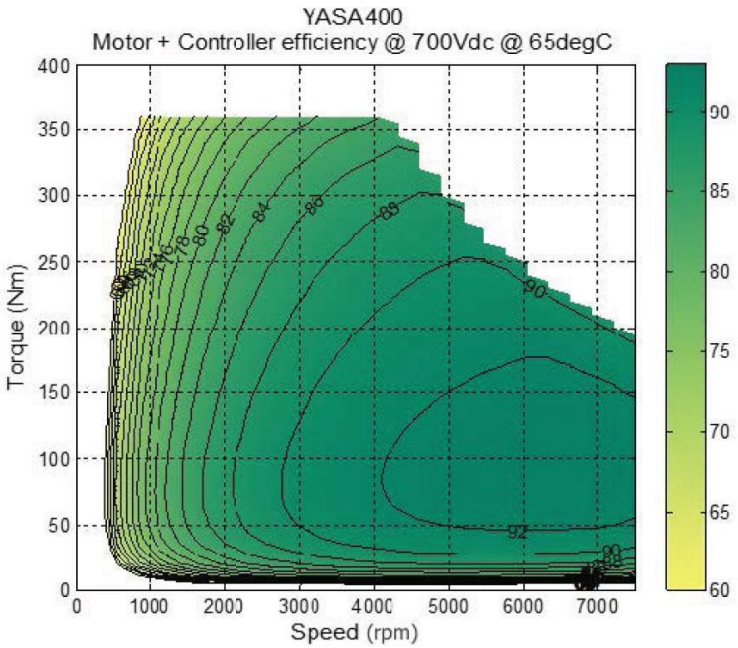

Figure 3.2: YASA 400 Motor Efficiency Map [17]

Since neither a specific motor model nor a motor efficiency map was provided, this project used the motor efficiency map for the YASA 400, which shares similar performance characteristics with the preexisting motor specifications. The data contained in the map were not numerically available, so the data needed to be extracted by image manipulation. Figure 3.3 shows the MATLAB numerical data obtained for the YASA 400 after image manipulation data extraction.

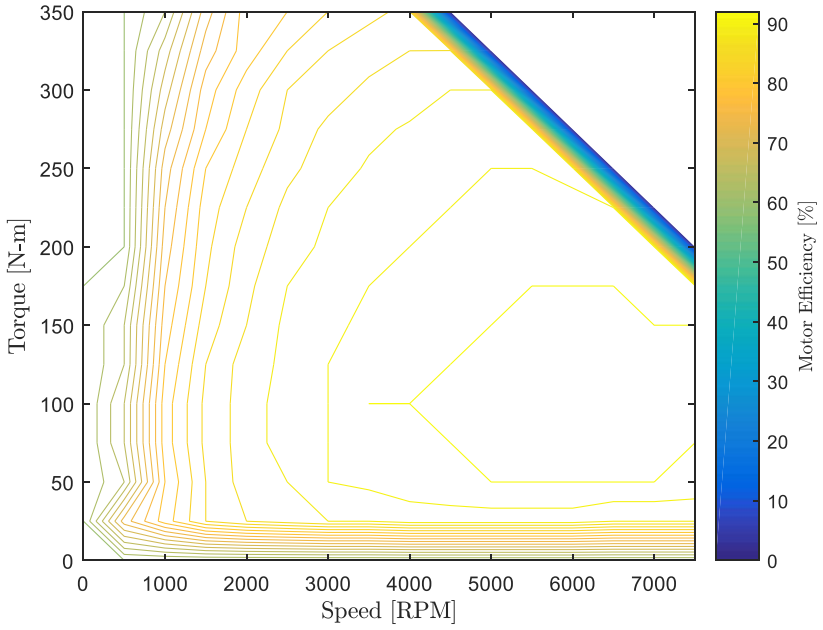

Figure 3.3: YASA 400 Extracted Efficiency Map

3.4.2 Application in Optimization Structure

3.4.2.1 Average Efficiency Computation

For each motor torque and rotational speed point for a given drive cycle and gear ratio, the corresponding motor efficiency, $\eta_m(t)$, can be extracted via 2D interpolation. As

such, the energy input into the motor needed to obtain the desired transmission output energy for a given drive cycle was given by the following equations:

$$P_i(t) = \frac{\tau_m(t)\omega_m(t)}{\eta_m(t)} \tag{3.11}$$

$$E_m = \sum_{t=0}^{T} P_i(\mathrm{t})\Delta t \tag{3.12}$$

As such, the average efficiency of the motor and transmission together over a given drive cycle could be computed as follows:

$$\eta = \frac{E_t}{E_m} \tag{3.13}$$

This average efficiency value was one of the critical outputs of the drive cycle simulation that was used in the optimization process.

3.4.2.2 Gear Ratio Upper and Lower Bounds

For a given drive cycle, the upper and lower bounds on feasible gear ratios are given by the following equations:

$$r_{lo} = \frac{\tau_{c,max}}{\tau_{m,max}} \tag{3.14}$$

$$r_{hi} = \frac{\omega_{m,max}}{\omega_{c,max}} \tag{3.15}$$

For a series of drive cycles, as is used in the optimization problem presented in this work, what may be within acceptable gear ratio bounds for one drive cycle may not work for

another drive cycle. As such, the bounds on all of the drive cycles combined needs to be combined as follows:

$$r_{lo} = \sup_{c \in \mathcal{C}} r_{lo,c} \tag{3.16}$$

$$r_{hi} = \inf_{c \in \mathcal{C}} r_{hi,c} \tag{3.17}$$

3.5 MOTOR NOISE MODEL

3.5.1 Motor Noise Data

Electric motor noise data, like transmission performance, requires a completed motor design and FEA analysis. These data are proprietary and are not publicly available, but the background research conducted found that the data are typically presented in the form of an acoustic spectrum, as shown in the MANATEE software output in Figure 3.4.

As neither a specific transmission model nor transmission acoustic data was provided, this project used the motor acoustic spectrum output given by the MANATEE software, shown in Figure 3.4. Via the same method of data extraction used to obtain the motor efficiency map for the YASA 400, the acoustic data contained in Figure 3.4 were extracted for use in this project. As the motor speed bounds for the MANATEE data were smaller than the motor speed bounds for the YASA 400, the bounds were adjusted to allow for performance analysis over the full speed range of the motor. The resulting acoustic spectrum is shown in Figure 3.5.

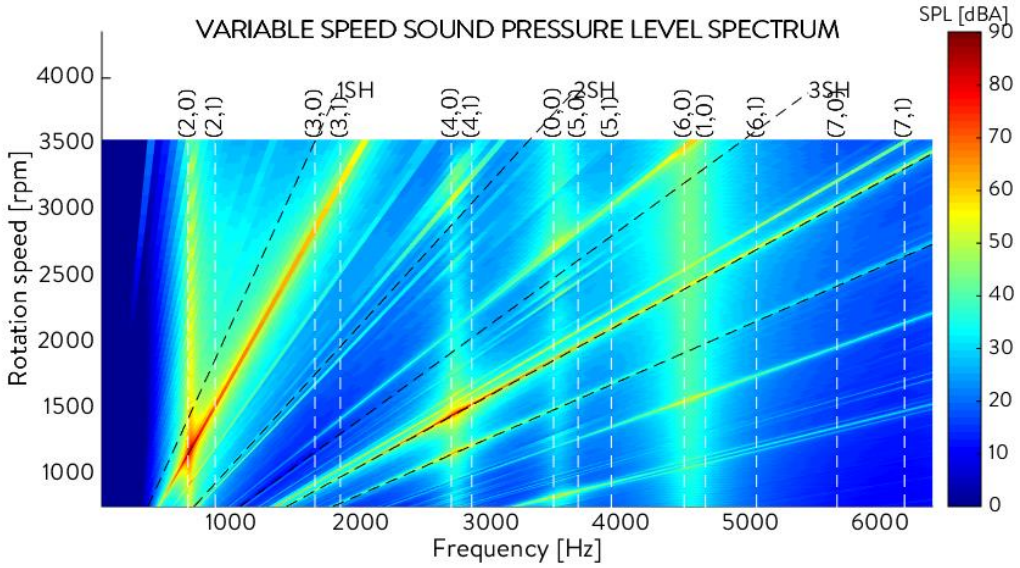

Figure 3.4: EOMYS MANATEE Acoustic Spectrum Output [18]

3.5.2 Application in Optimization Structure

As the primary concern for this project was the minimization of acoustic noise in general, rather than acoustic noise of a specific frequency, the acoustic spectrum was reduced in order by averaging the sound pressure level at all frequencies for each speed operating point. The resulting curve is shown in Figure 3.6.

For each motor speed point for a given drive cycle, the corresponding acoustic noise operating point was obtained using linear interpolation. To weight the average motor acoustic noise to match that of the average cycle efficiency, the average motor acoustic noise is normalized by dividing by the maximum possible sound pressure level, that is:

$$p_m = \frac{\overline{SPL_m}}{SPL_{m,max}} \tag{3.18}$$

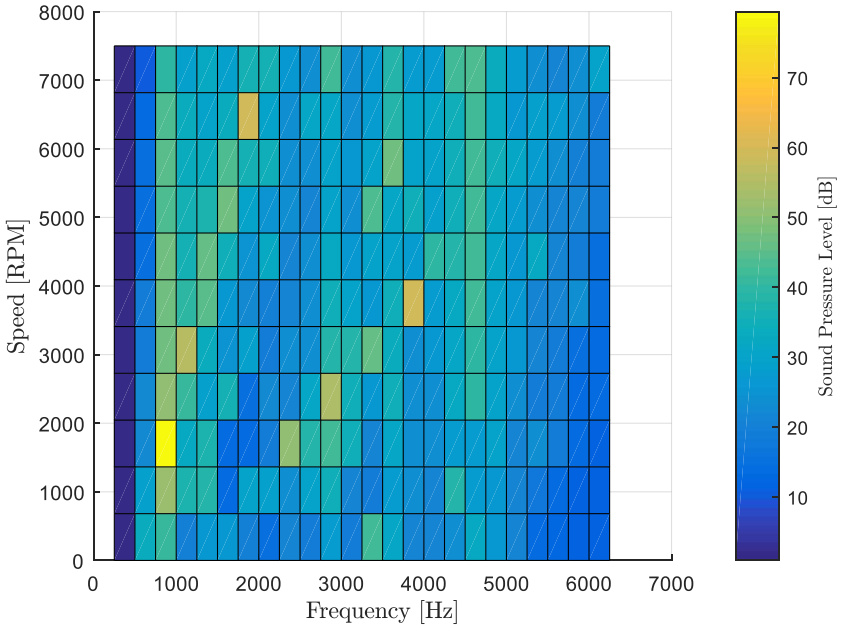

Figure 3.5: EOMYS MANATEE Extracted Acoustic Spectrum

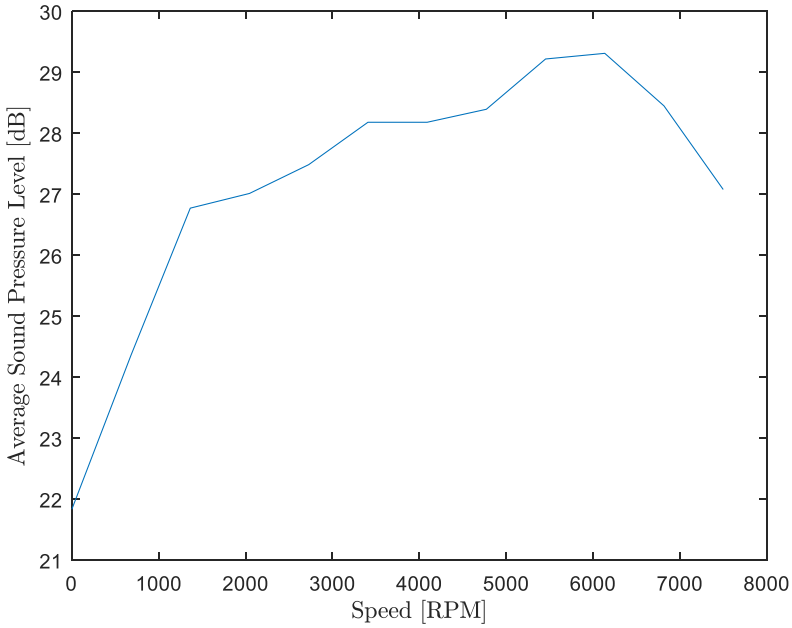

Figure 3.6: EOMYS MANATEE Extracted Average Sound Pressure Levels

The normalized average motor sound pressure level is the second critical output of the drive cycle simulation to be used in the cost function.

3.6 TRANSMISSION NOISE MODEL

3.6.1 Transmission Noise Data

Transmission noise data are typically provided as a function of transmission input torque and speed. In the case of this implementation, these are equivalent to τ_m and ω_m, respectively. Just like for the motor efficiency map and motor noise spectrum, these data are only available with the development of a full FEA model, which were not provided.

Fortunately, an undisclosed contact from a transmission design firm graciously provided two sources of proprietary transmission noise data. The data were not provided as numerical data, but rather as images of plots. These data were extracted by using GRABIT for MATLAB. The resulting transmission noise curve is shown in Figure 3.7. Since the data are proprietary, the z-axis of Figure 3.7 has been redacted. It must be noted, however, that the provided transmission noise data contained data points with negative sound pressure levels. In the context of the real world, these points signify that the transmission noise at each of these points is outside of the range of human hearing and would be inaudible to the human ear.

3.6.2 Application in Optimization Structure

For each motor torque and speed point for a given drive cycle, the corresponding transmission sound pressure level could be extracted via 2D interpolation and averaged across the drive cycle to obtain average sound levels. As was the case for motor noise, the sound pressure levels were normalized by the maximum possible sound pressure level:

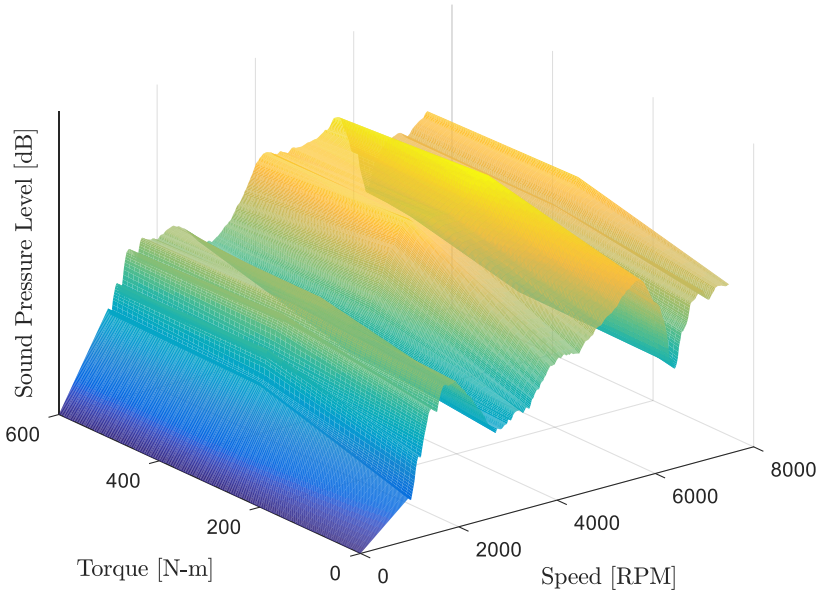

Figure 3.7: Extracted Transmission Acoustic Data

$$p_t = \frac{\overline{SPL_t}}{SPL_{t,max}} \tag{3.19}$$

Additionally, non-positive values were set to zero, since they lie outside of the range of human hearing and therefore should not affect the optimization computation. This normalized average transmission sound pressure level is the final output of the drive cycle simulation to be used in the cost function.

4 Methodology

4.1 Nelder-Mead Derivative-Free Optimization (1965) [15]

4.1.1 Overview

Given a set of m initial guess points in the feasible region for a function, $x_1, \dots, x_m$, where $m = (n + 1)$ if n is the dimension of the feasible region – i.e. $x_1, \dots, x_m \in \mathbb{R}^n$ – the Nelder-Mead simplex method provides an algorithmic way to obtain a locally optimal point for a derivative-free optimization problem defined as follows:

$$\begin{aligned} &\min f(x) \\ &\text{s.t. } x \in \mathcal{X} \subseteq \mathbb{R}^n \end{aligned} \tag{4.1}$$

Since the gradient of $f(x)$ cannot be computed, the direction of steepest descent cannot be identified without a global search in the region about a given point x. As such, gradient-based and Hessian-based methods of optimization – e.g. Newton's method – cannot solve this optimization problem. The Nelder-Mead simplex method procedurally seeks out a path of increased optimality or shrinks the simplex such that the problem will converge eventually to a locally optimal point by means of reflection, contraction, and expansion.

4.1.2 Procedure

Given a set of m points, as described previously, the Nelder-Mead algorithm sorts the points such that $f(x_1) \leq f(x_2) \leq \cdots \leq f(x_m)$ and computes a centroid of the points as follows:

$$x_c = \frac{1}{m-1} \sum_{i=1}^{m-1} x_i \tag{4.2}$$

Once the centroid is computed, the point of reflection of x_m is computed as follows with some $\alpha > 0$:

$$x_r = (1 + \alpha)x_c - \alpha x_m \tag{4.3}$$

4.1.2.1 Case 1: Reflection

If $f(x_1) \leq f(x_r) < f(x_{m-1})$, then x_m is replaced with x_r and the next iteration is run. That is, if the cost associated with x_r is between the lowest and second-highest costs of the given m points, then x_m should be removed from the set of m points and replaced with x_r before continuing with the next iteration.

4.1.2.2 Case 2: Expansion

If $f(x_r) < f(x_1)$, then a new minimum has been found and the search direction leads in a direction of decreasing cost. Continuing with this momentum, an expansion point is computed as follows with some $\gamma > 1$:

$$x_e = \gamma x_r + (1 - \gamma)x_c \tag{4.4}$$

If $f(x_e) < f(x_1)$, then the expansion step has found a better point of lower cost to expand the simplex and x_1 should be replaced with x_e. Otherwise, the expansion step has caused the system to reach a point that is not as good as x_r and so x_r should replace x_1 to continue the optimization process.

4.1.2.3 Case 3: External Contraction

If $f(x_{m-1}) \leq f(x_r) < f(x_m)$, then replacing x_m with x_r would not cause any other points to become a new maximum to improve the set of points for optimization.

Therefore, the new set of points should be a contraction of the reflected set. This is done by computing a new point of maximum cost as follows, with some $\beta \in (0, 1)$:

$$x_{ec} = \beta x_m + (1 - \beta) x_r \tag{4.5}$$

Once this point is obtained, x_m is replaced with x_{ec} and the algorithm proceeds to the next iteration.

4.1.2.4 Case 4: Internal Contraction

If $f(x_m) \leq f(x_r)$, then the reflection point does not improve the set of points of the algorithm and the current set of points should be shrunk to help with convergence. To do so, for every point x_i in the set, a new point x_i' should be computed as follows:

$$x_i' = \frac{1}{2}(x_1 + x_i) \tag{4.6}$$

This new set of x_i' are the set of m points with which the algorithm continues.

4.2 SOFTWARE IMPLEMENTATION

The Nelder-Mead simplex algorithm was chosen since it is already fully-implemented in MATLAB's optimization toolbox. The fminsearch function in MATLAB uses the Nelder-Mead simplex method to minimize a function given an initial guess. It is important to note that the fminsearch function does not permit the use of constraints and so an indicator function must be used. The indicator function for a feasible set $\mathcal{X}$ is defined as follows

$$I_{\mathcal{X}}(x) = \begin{cases} 0, & x \in \mathcal{X} \\ \infty, & x \notin \mathcal{X} \end{cases} \tag{4.7}$$

4.2.2 Cost Function

In the case of classical optimization problems, $f(x)$ is typically defined as a cost function $J(x)$, which assigns a cost to each of the possible outputs of a simulation. Both the single-speed and two-speed transmission optimization processes feature such a cost function, defined as follows:

$$J(x) = -k_{\eta} \sum_{c \in \mathcal{C}} \eta_c + k_{p_m} \sum_{c \in \mathcal{C}} p_{m,c} + k_{p_t} \sum_{c \in \mathcal{C}} p_{t,c} \tag{4.8}$$

For both the transmission noise and motor noise, a normalized value – rather than the raw value – is used. Since efficiency is upper- and lower-bounded by 1 and 0, respectively, using decibel values two orders of magnitude larger causes a scaling inaccuracy in the cost function computation for noise. Since each possible transmission and motor will have different upper and lower bounds on noise, no universal constant can be implemented to allow for this software to be used for any motor or transmission. Therefore, the software normalizes the average sound pressure level output by the maximum possible sound pressure levels of the transmission and motor so that any transmission and motor can be used.

4.3 Problem Formulation

The primary work and contribution of this thesis is the design of a framework in which a transmission's gear ratio can be optimized for efficiency and acoustic performance over a set of drive cycles given motor efficiency data and acoustic data for the motor and transmission. The following two sections provide an in-depth discussion in the formulation of the optimization problem for the single-speed and two-speed transmissions.

4.3.1 Single-Speed Transmission Optimization

In the case of the single-speed transmission, the only parameter to be optimized is the gear ratio of the transmission, which must lie within the acceptable range of gear ratios based on the drive cycles and motor. This problem can be written in standard form as follows:

$$\min_x J(x) \qquad (4.9)$$
$$\text{s.t. } x \in \mathcal{X} = \{x : r_{lo} \leq x \leq r_{hi}, x \in \mathbb{R}\}$$

Since fminsearch cannot accept constraints on the input variables, the problem must be reformulated with an indicator function as such

$$\min_x [J(x) + I_{\mathcal{X}}(x)] \qquad (4.10)$$

Inputting $J(x) + I_{\mathcal{X}}(x)$ to be minimized in fminsearch yields a locally optimal gear ratio for a given set of drive cycles, motor, and transmission.

As will be discussed in Chapter 5, although fminsearch finds a locally optimal gear ratio, in this application of the algorithm, fminsearch locates a globally optimal gear ratio for the transmission. Firstly, as was discovered, the cost function for the data sets studied is convex. That is, for the data sets,

$$J(\lambda x_1 + (1-\lambda)x_2) \leq \lambda J(x_1) + (1-\lambda)J(x_2) \qquad (4.11)$$
$$\forall x_1, x_2 \in \mathcal{X}$$
$$\forall \lambda \in [0, 1]$$

Based on the nature of convex functions, any locally optimal solution is also a global solution and so fminsearch locates the globally optimal solution. However, while the cycles studied have convex cost functions, it may not be generally true for all combinations of drive cycles, motors, and transmissions. As such, the midpoint for the upper and lower bounds on the gear ratio is used as an initial guess. That is,

$$x_0 = \frac{r_{hi} + r_{lo}}{2} \tag{4.12}$$

Choosing such a point has successfully yielded globally optimal operating points due to the fact that motors and transmissions tend to demonstrate better performance in the middle range of its operable region, rather than at the extrema.

4.3.2 Two-Speed Transmission Optimization

In the case of the two-speed transmission, not only do the two gear ratios need to be optimized, but for any given pair of gear ratios, there is a switching point that needs to be optimized. Additionally, each of the two gear ratios must lie within the feasible region for gear ratios and the switching point must lie within the operational speed limits of the motor. Stated in standard form,

$$\begin{aligned} &\min_{x_1,x_2} \min_{\omega_s} J(x_1, x_2, \omega_s) \\ &\text{s.t. } x_1, x_2 \in \mathcal{X} = \{x : r_{lo} \leq x \leq r_{hi}, x \in \mathbb{R}\} \\ &\qquad \omega_s \in \Omega = \left\{\omega : \omega_{m,min} \leq \omega_s \leq \omega_{m,max}, \omega_s \in \mathbb{R}\right\} \end{aligned} \tag{4.13}$$

As in the one-speed transmission optimization, fminsearch cannot take in any constraint arguments to bound the gear ratios or the switching point. Thus, the problem must be

reformulated as follows:

$$\min_{x_1,x_2} \min_{\omega_s} [J(x_1, x_2, \omega_s) + I_X(x_1) + I_X(x_2) + I_\Omega(\omega_s)] \tag{4.14}$$

4.3.2.1 MATLAB Implementation

Since this is a two-fold optimization, the implementation in MATLAB features the use of a nested optimization with fminsearch. The internal optimization is done by a function called optSwpt, which uses fminsearch to minimize $J(x_1, x_2, \omega_s)$ by changing ω_s within feasible switching point bounds for a fixed pair of gear ratios, x_1 and x_2. This function then returns the optimal switching point, ω_s^*, and the associated minimized cost, $J(x_1, x_2, \omega_s^*)$.

The external minimization is conducted by a function called optGears, which uses fminsearch to minimize the cost returned by optSwpt, $J(x_1, x_2, \omega_s^*)$, by changing x_1 and x_2 within feasible gear ratio bounds. This function returns the optimal gear ratios, x_1^* and x_2^*, and the associated minimized cost, $J(x_1^*, x_2^*, \omega_s^*)$, which is the minimum cost for the overall optimization problem.

In optimizing the switching point, an initial guess of a switching point at the midpoint of the motor's operational bounds is used. That is,

$$\omega_{s,0} = \frac{\omega_{m,max} + \omega_{m,min}}{2} \tag{4.15}$$

For the switching point optimization, choosing the midpoint presents an ideal initial guess, since the transmission is about as likely to be operating in low gear as it is in high gear. At significantly higher or lower switching points, the motor tends to operate in one gear ratio

more so than the other. This formulation found the globally optimal switching point in all of the cases studied, as will be presented in Chapter 5.

4.3.2.2 Difficulties and Solutions for Gear Ratio Optimization

Initially, the optimization algorithm used the midpoint of the feasible gear ratios as the initial guesses for the gear ratio optimization process. That is,

$$x_{1,0} = x_{2,0} = \frac{r_{hi} + r_{lo}}{2} \tag{4.16}$$

However, when compared to the brute-force search optimal solution, it was found that the optimal gear ratios returned by fminsearch, x_1^* and x_2^*, were suboptimal. Further analysis showed that there were two local optima in the search space for the gear ratios.

To remedy this issue, a coarse global search across the search space was used to identify a good initial guess for x_1 and x_2. Implementing this initial step allowed fminsearch to locate the global minimum and still yielded a computation time significantly shorter than that required for a global search.

5 Results and Discussion

5.1 Input Parameters

This implementation of gear ratio optimization used a set of six drive cycles, extracted from NREL's ADVISOR software and smoothed as discussed in Chapter 3. The six drive cycles were chosen because they best demonstrated the ability to improve efficiency and reduce noise when compared to Shuguang's proposed ratio. The cycles are as follows:

- 1.65-mile Bus Route with 28 Stops
- Manhattan Bus Drive Cycle
- New York City Cycle
- New York City Garbage Truck Cycle
- New York City Bus Cycle
- London Bus Route

The vehicle specifications used are those provided by Shuguang for an unloaded vehicle and are detailed in Appendix B. As a placeholder motor, this implementation uses the YASA 400 efficiency data and the adjusted EOMYS MANATEE sound spectrum. For transmission noise performance, the acoustic data from the undisclosed source were used.

5.2 Cost Function Weights

In analyzing the performance of the optimization algorithm, this study considered three primary cases, shown in Table 5.1. Each of these cases was run through the optimization software to determine an optimal operating point for a one-speed transmission and a two-speed transmission. The results are discussed in the following sections.

Case	k_η	k_{p_m}	k_{p_t}
Balance Efficiency and Noise	1.0	0.5	0.5
Maximize Efficiency	1.0	0.0	0.0
Minimize Noise	0.0	1.0	1.0

Table 5.1: Optimization Study Cases

5.3 One-Speed Transmission

5.3.1 Results

Running the optimization algorithm using the fminsearch formulation completed in approximately 0.934 seconds, compared to the brute-force search program runtime of 2.042 seconds. The resulting gear ratios and performance indicators are shown in Appendix D.

5.3.2 Validation

In assessing the validity of the optimization algorithm for each of the three cases, a comparison against the brute-force search algorithm result was used. The results are shown in Figures 5.1-5.3 for each of the three cases. In all three cases observed, fminsearch successfully located the globally optimal operating point and was able to do so in a significantly shorter period of time and in fewer cost function computations.

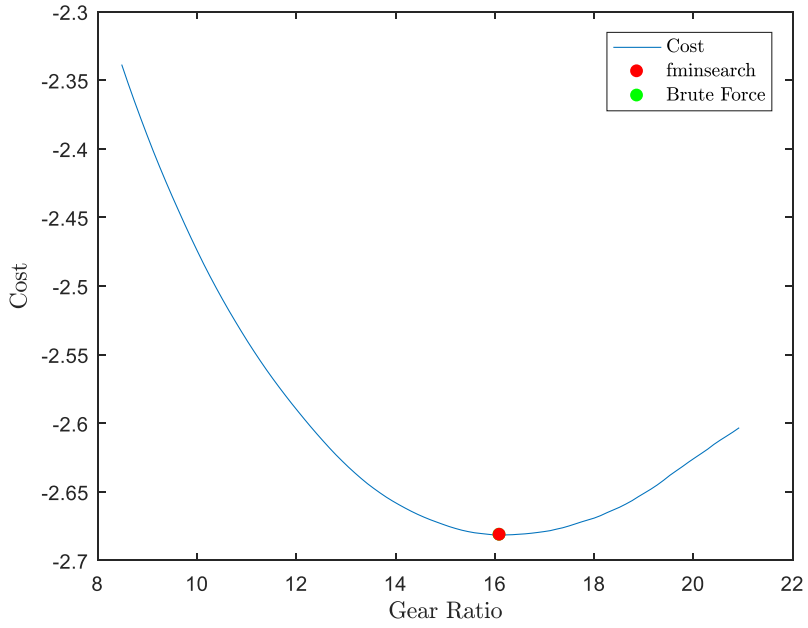

Figure 5.1: Optimization Results for One-Speed Balanced Case

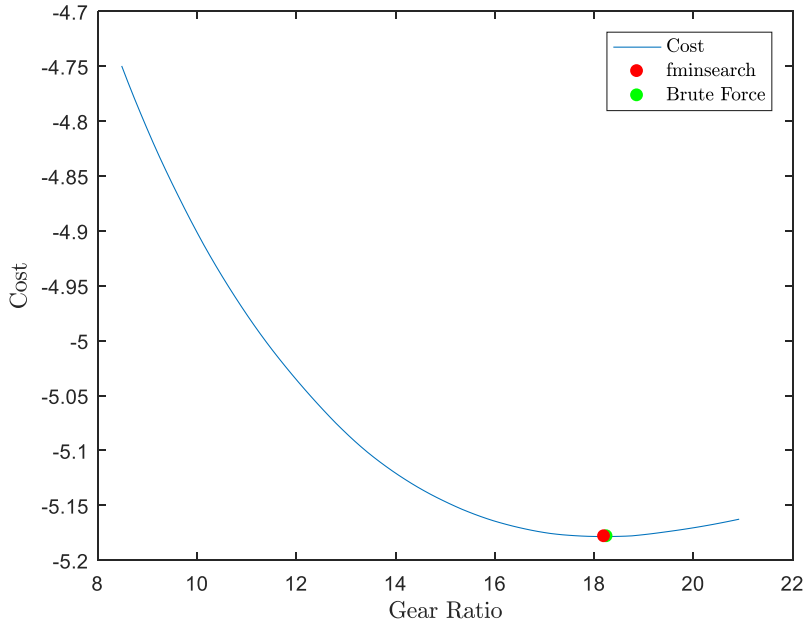

Figure 5.2: Optimization Results for One-Speed Max Efficiency Case

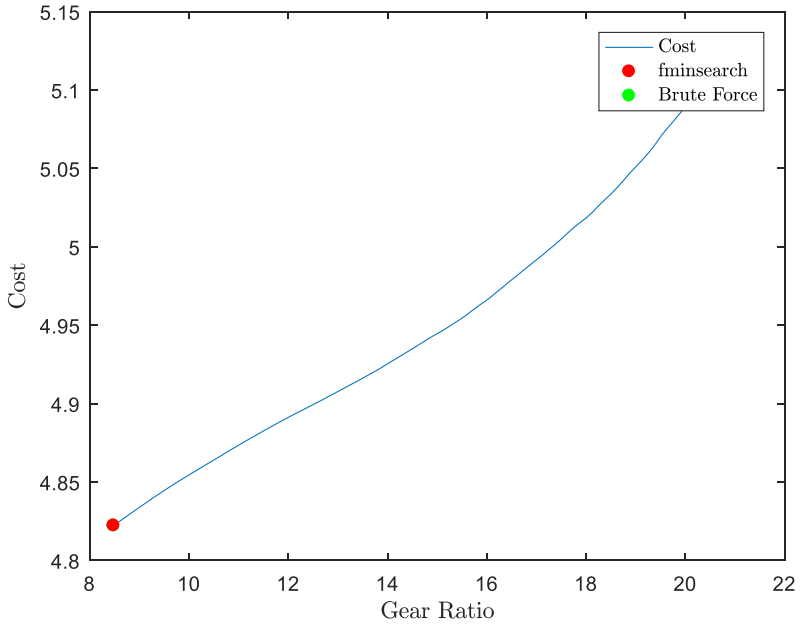

Figure 5.3: Optimization Results for One-Speed Noise Minimization Case

5.3.3 Discussion

5.3.3.1 Efficiency Improvement

In the case where the software optimizes for efficiency, the program identifies an upper bound for efficiency at 86.31%, giving a maximum possible efficiency improvement of 5.39 percentage points. This improvement comes at a cost of a 2.66 dB increase in transmission noise and a 0.62 dB increase in motor noise.

5.3.3.2 Noise Reduction

Based on the results presented in Appendix D, it is clear that while an improvement in average efficiency of at least three percentage points is possible, a decrease in transmission and motor noise of at least three decibels is infeasible. With the given set of

drive cycles, the best-case scenario for average sound pressure level drop is a small 0.68 dB.

Considering that the efficiency and acoustic performance of the drivetrain is heavily dependent on drive cycle specifications, a survey of all of NREL's ADVISOR drive cycles was conducted to identify if any of them could yield a drop in average sound pressure level of at least three decibels. Of the 40 possible drive cycles, only ten demonstrated an ability to reduce noise levels by at least three decibels, but at the cost of at least eight percentage points in efficiency, with the stop frequency and maximum speed of each cycle having a significant impact on noise production. As such, it has been recommended that a drive cycle that more closely reflects the demands for their vehicle's application be developed and for the optimization to be conducted over such a cycle, which could yield better results, depending on its nature.

Most critically to note is that in all of the cases, the average transmission sound pressure levels lie in the inaudible region of the sound spectrum. That is, the average transmission sound pressure level in all cases is less than zero and cannot be heard by human ears, though at individual time points, it may cross over into the audible region.

5.3.3.3 Better Performance at Equal Sound Levels

The results of the efficiency maximization and noise reduction optimization processes raised the question of whether or not a point of equivalent noise production but greater performance efficiency was possible. Of the 40 cycles studied, only five cycles showed the potential for equivalent or better acoustic performance at a higher efficiency. In the other 35 cycles studied, noise and gear ratio both increase with gear ratio, so any improvement in efficiency causes an increase and noise and any improvement in noise causes a decrease in efficiency.

The five drive cycles for which equivalent noise performance with greater efficiency is possible are the central business district cycles, the Japan 10-15 cycle, the ECE cycle, and the bus route cycle. For the two central business district cycles, a significant improvement in noise performance is possible at greater efficiency performance, while for the other three cycles, only marginally better or equivalent acoustic performance can be achieved. The efficiency and transmission noise plots are shown in Figures 5.4-5.8.

Based on these results, the ability to demonstrate improvement in efficiency and noise is dependent on the drive cycle demands for the vehicle. Further research or the construction a set of drive cycles that more accurately reflect the predicted vehicle demands is recommended.

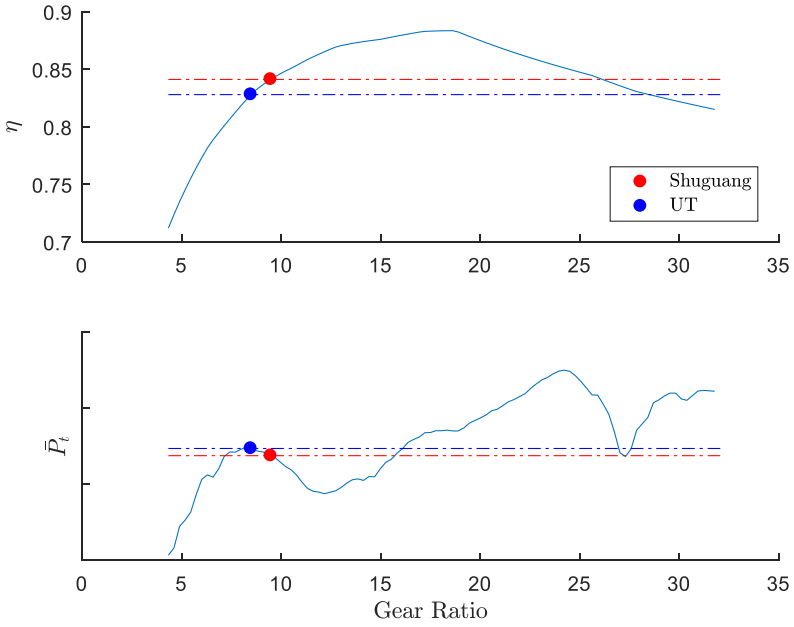

Figure 5.4: Efficiency and Average Transmission Sound Pressure Level for CBD 14

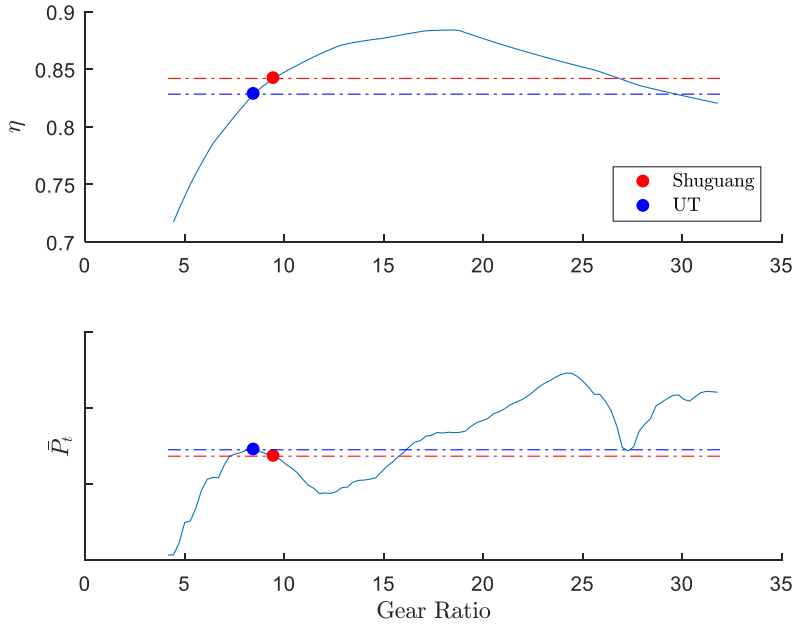

Figure 5.5: Efficiency and Average Transmission Sound Pressure Level for CBD Bus

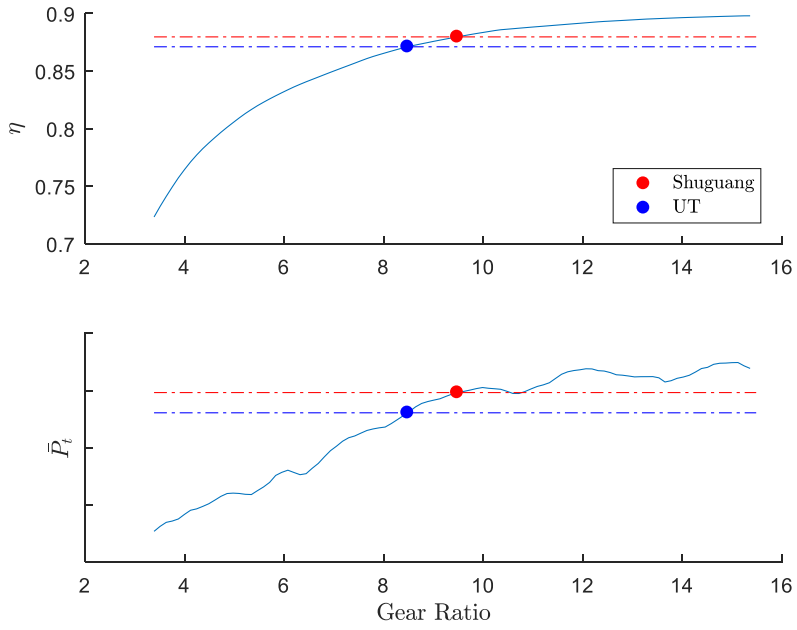

Figure 5.6: Efficiency and Average Transmission Sound Pressure Level for Japan 10-15

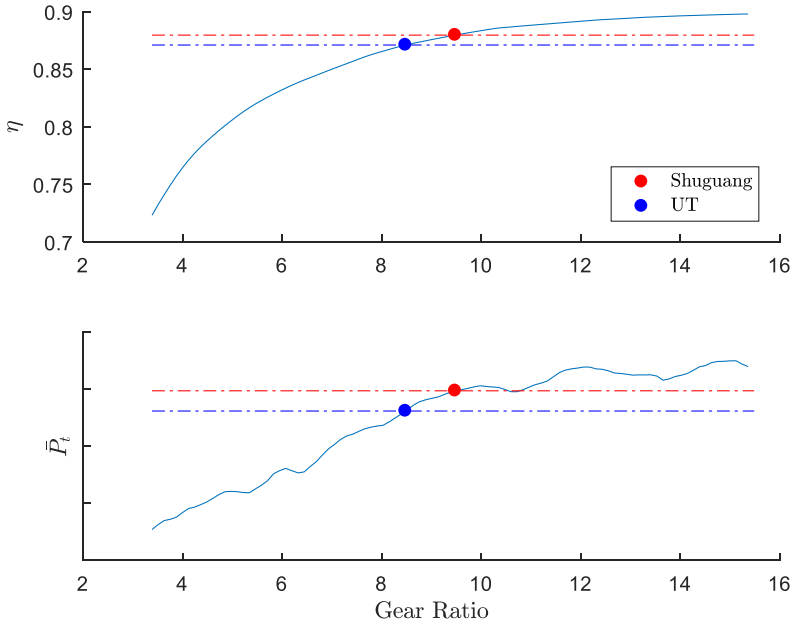

Figure 5.7: Efficiency and Transmission Sound Pressure Level for ECE Cycle

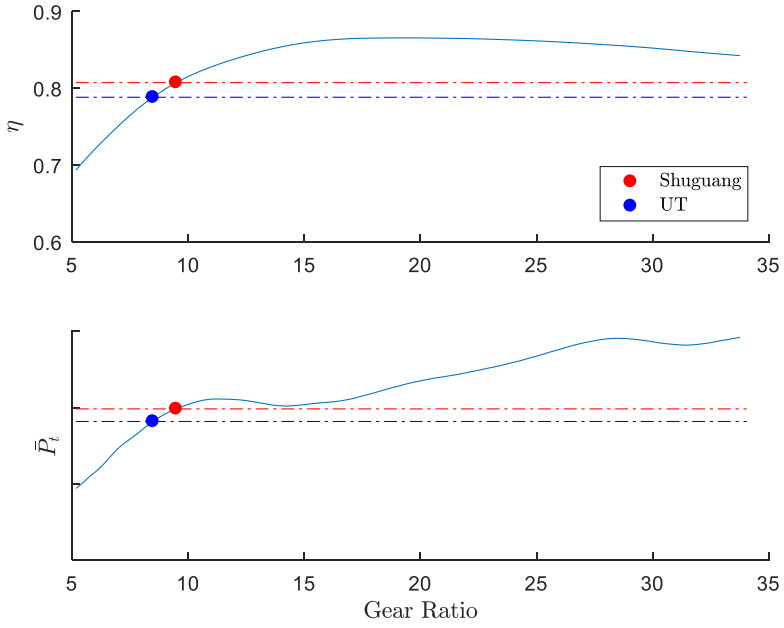

Figure 5.8: Efficiency and Average Sound Pressure Level of Bus Route Cycle

5.4 TWO-SPEED TRANSMISSION

5.4.1 Results

Running the optimization algorithm using the fminsearch formulation completed in approximately 146 seconds, compared to the brute-force search program runtime of 5,567.751 seconds. The resulting gear ratios, switching points, and performance indicators are shown in Appendix E.

5.4.2 Validation

5.4.2.1 Switching Point

In assessing the validity of the algorithm for each of the switching point optimization problems, a comparison against the brute-force search algorithm result was used. The results are shown in Figures 5.9-5.10 for each case. In all of the cases observed, fminsearch successfully located the globally optimal operating point and was able to do so in a significantly shorter period of time and in significantly fewer cost function computations.

It should also be noted that in the noise minimization case, both the high and low gear ratios are the same. That is, only one gear ratio is sufficient and there is therefore no need for a switching point.

5.4.2.2 Gear Ratios

In assessing the validity of the algorithm for each of the three cases, a comparison against the brute-force search algorithm result was used. The results are shown in Figures 5.11-5.13 for each case. In all of the cases observed, fminsearch successfully located the globally optimal operating point and was able to do so in a significantly shorter period of time and in fewer cost function computations.

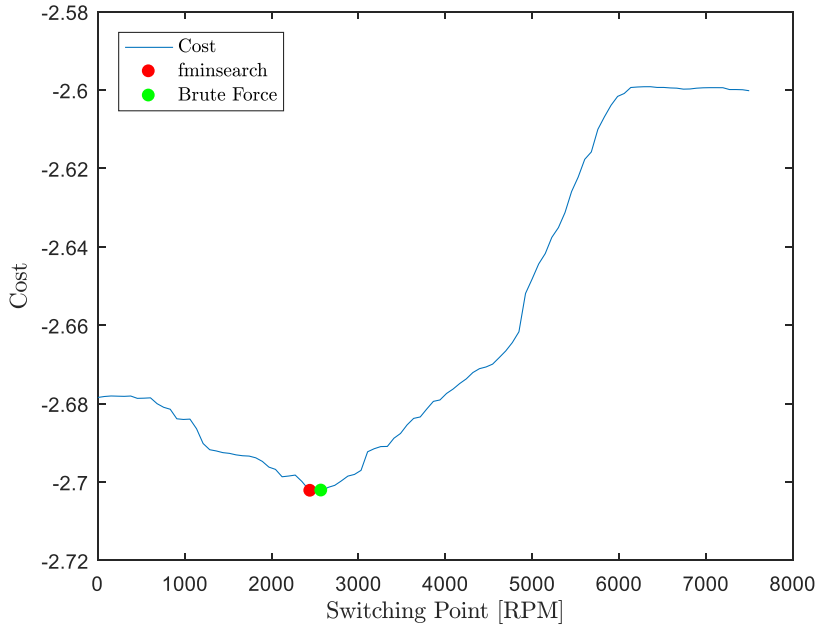

Figure 5.9: Switching Point Optimization Result for Two-Speed Balanced Case

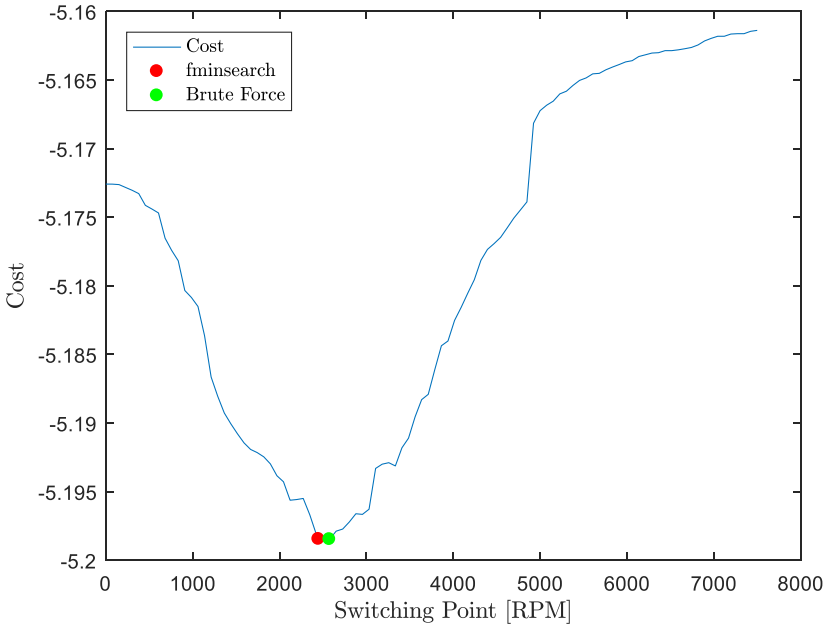

Figure 5.10: Switching Point Optimization Result for Two-Speed Max Efficiency Case

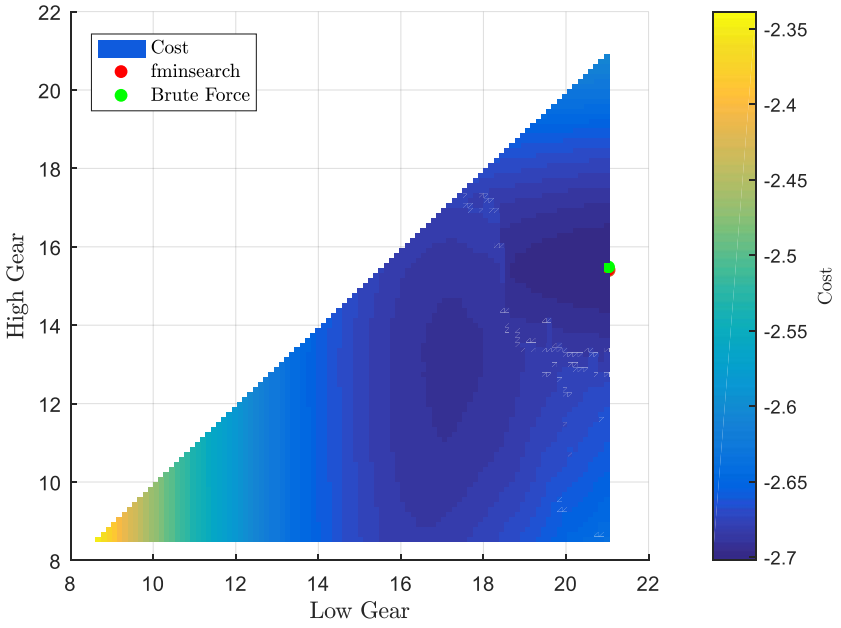

Figure 5.11: Optimization Results for Two-Speed Balanced Case

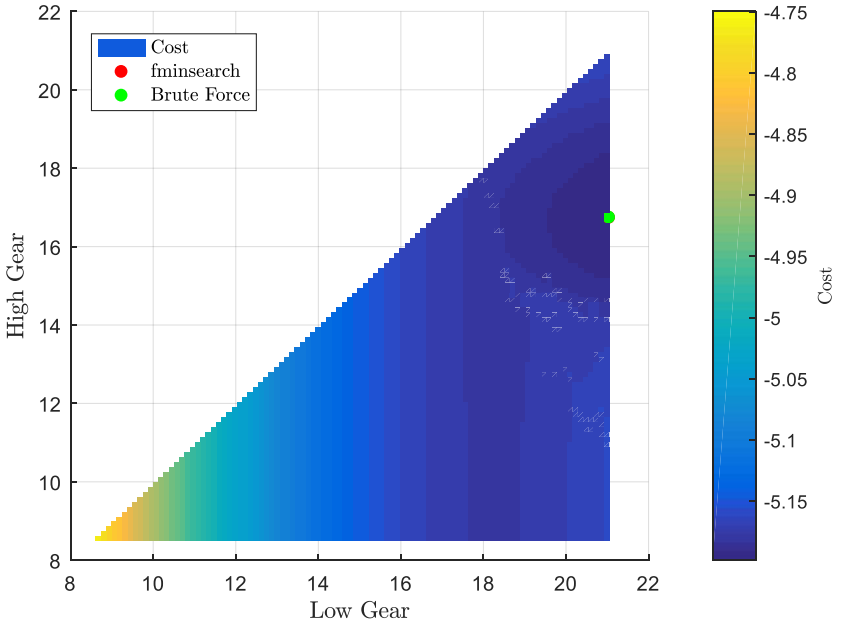

Figure 5.12: Optimization Results for Two-Speed Max Efficiency Case

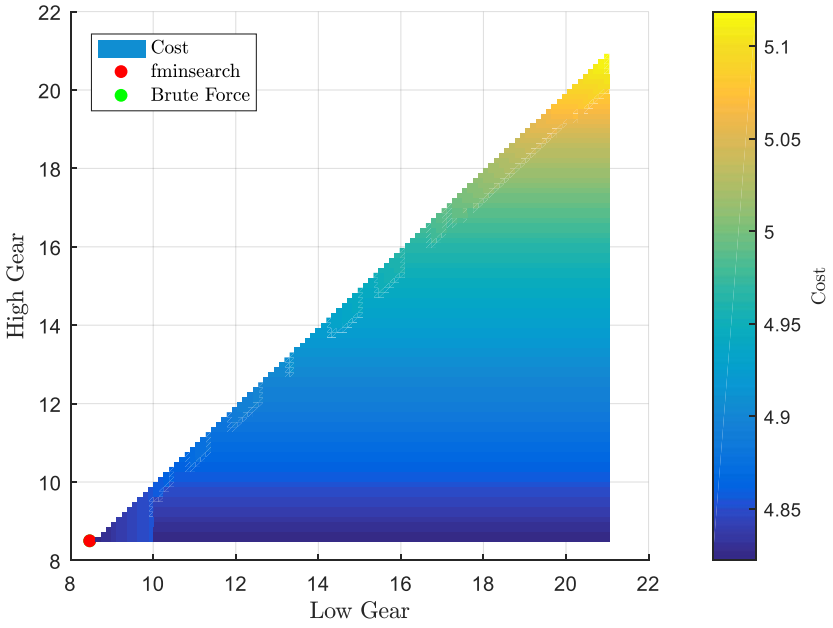

Figure 5.13: Optimization Result for Two-Speed Noise Minimization Case

5.4.3 Discussion

Based on the results presented in Appendix E, the maximum achievable efficiency improvement brings the efficiency up to 86.64%, which provides a 5.72 percentage point increase in performance over the originally proposed gear ratio and a 0.33 percentage point increase in performance over the efficiency-maximized optimal single-speed gear ratio. This, however comes at a cost of a three decibel increase in transmission noise compared to the proposed transmission design and 0.34 dB increase when compared to the efficiency-maximized optimal single-speed gear ratio.

It should be noted that not only is there only a marginal improvement efficiency for adding a second gear ratio, there also exists the potential incurred cost in inefficiencies in shifting, production and assembly cost, and malfunction due to complexity. Due to the

already highly-efficient characteristics of electric motors, it was recommended that a two-speed transmission was not favorable in the current market when compared to a well-optimized single-speed transmission.

6 Conclusion

6.1 Contribution to Field

To this point, no prior work has been found that developed a framework for optimizing transmission performance for both efficiency and acoustic noise in electric vehicles. This project creates the groundwork for developing a method of optimizing transmission design for use in electric vehicles when taking into account acoustic performance as well. As electric motors become increasingly advanced to where an efficiency improvement as small as 0.1 percentage point provides a competitive edge, designing two- and multi-speed transmissions will be crucial to improve performance of such vehicles.

Additionally, the effects of the high-efficiency nature of electric motors on vehicle performance and the economic benefit of designing multi-speed transmissions have been studied. Even across multiple use cases and gear ratios, drivetrain efficiency for these vehicles is significantly higher than for internal combustion engine vehicles. As such, until the market fully adopts electric vehicles, the marginal gain in performance achieved by adding additional gear ratios to the transmission may not outweigh the costs of developing, producing, and maintaining a more complex transmission.

Finally, this work provides a study into the relationship between motor efficiency, motor noise, and transmission noise. Namely, given the present design and models available, the three parameters of interest seem to increase together with respect to increasing gear ratio.

6.2 Future Work

To continue with this project, the implementation of advanced motor and transmission FEA models is proposed. In all of the background research done to create this

product, the most commonly identified issue was the lack of FEA model outputs to provide accurate information regarding acoustic performance. Additionally, an implementation of inefficiency computations within the transmission should be included. Since gear teeth do not mesh perfectly in a transmission, there is energy loss due to friction that has not been accounted for in this project.

Appendices

APPENDIX A SHUGUANG VEHICLE PARAMETERS

Parameter	Value
Length x Width x Height [mm]	6105 x 2025 x 2820
Wheelbase [mm]	3715
Front Track [mm]	1716
Rear Track [mm]	1732
Minimum Ground Clearance [mm]	198
Effective Tire Radius [mm]	365

Table A-1: Shuguang Vehicle Dimensions

Parameter	Value
Maximum Weight [kg]	4460
Maximum Front Axle Static Load [kg]	1960
Maximum Rear Axle Static Load [kg]	2500
Unloaded Weight [kg]	3033
Unloaded Front Axle Static Load [kg]	1508
Unloaded Rear Axle Static Load [kg]	1525
Load Capacity [kg]	1427

Table A-2: Shuguang Vehicle Weight and Load Specifications

Parameter	Value
Maximum Velocity [km/h]	140
Maximum Cruise Velocity [km/h]	100
Maximum Road Grade [%]	20

Table A-3: Shuguang Vehicle Performance Demands

Parameter	Value
Motor Type	Permanent-Magnet Synchronous Motor
Motor Cooling	Water-Cooled
DC Motor Voltage [V]	350
Continuous Power [kW]	60
Peak Power [kW]	120
Continuous Torque [N-m]	175
Peak Torque [N-m]	450
Maximum Velocity [RPM]	9650
Proposed Gear Ratio	9.4788

Table A-4: Shuguang Vehicle Powertrain Specifications

APPENDIX B OPTIMIZATION SIMULATION PARAMETERS

Parameter	Value
Frontal Area [m^2]	5.7105
Drag Coefficient	0.51
Rear Axle Load [kg]	1525
Total Mass [kg]	3033
Rolling Friction Coefficient	0.03
Tire Static Friction Coefficient	1.00
Tire Radius [m]	0.365

Table B-1: Unloaded Vehicle Parameters Used for Simulation

Parameter	Value
Frontal Area [m^2]	5.7105
Drag Coefficient	0.51
Rear Axle Load [kg]	2500
Total Mass [kg]	4460
Rolling Friction Coefficient	0.03
Tire Static Friction Coefficient	1.00
Tire Radius [m]	0.365

Table B-2: Loaded Vehicle Parameters Used for Simulation

APPENDIX C NREL DRIVE CYCLES

WVU 5-Peak Truck Cycle	NREL to Vail, CO
Japanese 10-15 Mode	New York City Cycle
Japanese 10-15 Prius Test	New York City Composite Cycle
ARB02 for Los Angeles Car Chases	New York City Truck Cycle
ARTERIAL	New York City Garbage Truck Cycle
1.65-mile Bus Route with 28 Stops	New York City Bus Cycle
Central Business District (CBD) 14-Stop	Nuremberg Bus Route 36
Central Business District (CBD) Bus	Orange County Cycle
Formula Electric Cleveland '97	REP05
COMMUTER	US EPA SC03
City-Suburban Heavy Vehicle Route	US EPA Urban Dyno Cycle
ECE	US EPA Urban Dyno for Heavy-Duty
EUDC	London Bus Route
ECE and EUDC for Low-Power Vehicles	UNIF01
US EPA Acceleration Stress Test	US EPA US06
US EPA Highway Fuel Economy	US EPA US06 Highway Cycle
US EPA Inspection and Maintenance 240	Vail, CO to NREL
INRETS – New European Drive Cycle	West Virginia City Cycle
CARB LA92	West Virginia Interstate Cycle
Manhattan Bus Drive Cycle	West Virginia Suburban Cycle

Table C-1: List of ADVISOR Drive Cycles

APPENDIX D ONE-SPEED OPTIMIZATION RESULTS

Case	Gear Ratio	Avg. η [%]	Avg. SPL_t Drop [dB]	Avg. SPL_m [dB]
Shuguang	9.4788	80.92	---	23.66
UT Balanced	16.1008	86.10	-1.98	24.16
UT Max Efficiency	18.2052	86.31	-2.66	24.28
UT Min Noise	8.4804	79.16	0.68	23.56

Table D-1: One-Speed Transmission Optimization Results

APPENDIX E TWO-SPEED OPTIMIZATION RESULTS

Case	Low Gear	High Gear	ω_s [RPM]	Avg. η [%]	Avg. SPL_t Drop [dB]	Avg. SPL_m [dB]
Shuguang	9.4788	---	---	80.92	---	23.66
UT Balanced	21.0499	15.3879	2449	86.56	-2.97	24.27
UT Max Efficiency	21.0499	16.7275	2449	86.64	-3.00	24.31
UT Min Noise	8.4804	8.4804	---	79.16	0.68	23.56

Table E-1: Two-Speed Transmission Optimization Results

Glossary

A	frontal area of vehicle [m^2]
a	vehicle acceleration [m/s^2]
C_d	aerodynamic drag coefficient []
$\mathcal{C}$	set of drive cycles used for optimization []
E_m	motor energy input [J]
E_t	transmission energy output [J]
η_c	average efficiency of a given drive cycle, c []
g	gravitational constant [9.81 m/s^2]
J	cost []
k_η	cost function efficiency weighting coefficient []
k_{p_m}	cost function normalized motor sound pressure level coefficient []
k_{p_t}	cost function normalized transmission sound pressure level coefficient []
M	total vehicle mass [kg]
μ_r	tire rolling friction coefficient []
p_m	normalized average motor sound pressure level []
p_t	normalized average transmission sound pressure level []
R	tire radius [m]
r_0	initial guess for gear ratio optimization []
r	gear ratio []
r_{hi}	gear ratio upper bound []
r_{lo}	gear ratio lower bound []
ρ	density of air [kg/m^3]
$\overline{SPL}_m$	average motor sound pressure level [dB]

$\overline{SPL_t}$	average transmission sound pressure level [dB]
$SPL_{m,max}$	maximum motor sound pressure level [dB]
$SPL_{t,max}$	maximum transmission sound pressure level [dB]
Δt	time step [s]
τ_a	torque required to accelerate vehicle [N-m]
τ_d	torque required to overcome aerodynamic drag [N-m]
τ_f	torque required to overcome road friction [N-m]
τ_m	motor output torque [N-m]
τ_t	transmission output torque [N-m]
V	vehicle velocity [m/s]
ω_m	motor output speed [RPM]
ω_s	switching point for a two-speed transmission [RPM]
ω_t	transmission output speed [RPM]

References

[1] Brooker, A., Haraldsson, K., Hendricks, T., Johnson, V., Kelley, K., Kramer, B., Markel, T., O'Keefe, M., Sprik S., Wipke, K., & Zolot, M. (2003). Advanced Vehicle Simulator (ADVISOR) [Software]. Available from http://adv-vehicle-sim.sourceforge.net/

[2] Hambley, A.R. (2014). *Electrical Engineering: Principles and Applications* (6th ed.). Upper Saddle River, NJ: Pearson Education, Inc.

[3] Bösing, M. (2013). *Acoustic Modeling of Electrical Drives: Noise and Vibration Synthesis based on Force Response Superposition* (Doctoral Dissertation).

[4] Andrej, M.F., & Boltezar, C.M. (2003). A coupled electromagnetic-mechanical-acoustic model of a DC electric motor. *COMPEL, 22*, 1155-1165. http://dx.doi.org/10.1108/03321640310483075

[5] Dupont, J., Aydoun, R., & Bouvet, P. (2014). Simulation of the Noise Radiated by an Automotive Electric Motor: Influence of the Motor Defects. *SAE International, 3(2)*, 310-320. doi:10.4271/2014-01-2070

[6] Islam, R., & Husain, I. (2010). Analytical Model for Predicting Noise and Vibration in Permanent-Magnet Synchronous Motors. *IEEE Transactions on Industry Applications, 46(6)*, 2346-2354. doi: 10.1109/TIA.2010.2070473

[7] Le Besnerais, J., Lanfranchi, V., Hecquet, M., Brochet, P., & Friedrich, G. (2010). Prediction of audible magnetic noise radiated by adjustable speed drive induction machines. *IEEE Transactions on Industry Applications, 46(4)*, 1367-1373. doi: 10.1109/TIA.2010.2049624

[8] Knöfel, B., Troge, J., & Drossel, W. G. (2016). Transmission Acoustics Between End-of-Line Testing and Vehicle Rating. *ATZextra worldwide, 21(1)*, 6-9. doi:10.1007/s40111-016-0007-z

[9] Williams, J. S., Steyer, G. C., & Ditman, J. (1996). Transmission Tonal Noise: Experimental Analysis of the NVH Characteristics Which Influence Vehicle Sound Quality. *The International Society for Optical Engineering*, 140-146.

[10] Tuma, J. (2009). Gearbox Noise and Vibration Prediction and Control. *International Journal of Acoustics and Vibration, 14(2)*, 1-11.

[11] Choi, J. S., Lee, H. A., Lee, J. Y., Park, G. J., Park, J., Lim, C. H., & Park, K. J. (2011). Structural optimization of an automobile transmission case to minimize radiation noise using the model reduction technique. *Journal of Mechanical Science and Technology, 25(5)*, 1247-1255. doi:10.1007/s12206-011-0135-3

[12] Morgan, J. A., Dhulipudi, M. R., Yakoub, R. Y., & Lewis, A. D. (2007). Gear Mesh Excitation Models for Assessing Gear Rattle and Gear Whine of Torque Transmission Systems with Planetary Gear Sets. *SAE Technical Paper.* doi:10.4271/2007-01-2245

[13] Hooke, R. & Jeeves, T.A. (1961). "Direct Search" Solution of Numerical and Statistical Problems. *Journal of the ACM, 8(2)*, 212-229. doi:10.1145/321062.321069

[14] Conn, A.R., Scheinberg, K., & Vincent, L.N. (2009). *Introduction to Derivative-Free Optimization*. Society for Industrial and Applied Mathematics.

[15] Nelder, J.A., & Mead, R. (1965). A simplex method for function minimization. *The Computer Journal, 7(4)*, 308-313. https://doi.org/10.1093/comjnl/7.4.308

[16] Rios, L.M., & Sahinidis, N.V. (2012). Derivative-free optimization: a review of algorithms and comparison of software implementations. *Journal of Global Optimization, 56(3)*, 1247-1293. doi:10.1007/s10898-012-9951-y

[17] YASA Motors, Ltd. (2015). *YASA-400 Axial Flux Electric Motor*. Retrieved from http://www.yasamotors.com/wp-content/uploads/2015/09/YASA-400-Product-Sheet.pdf

[18] EOMYS. [Variable Speed Sound Pressure Level Spectrum]. *Magnetic Acoustic Noise Analysis Tool for Electrical Engineering*. Retrieved from http://www.eomys.com/produits/manatee/article/logiciel-manatee?lang=en

[19] Gao, B., Liang, Q., Xiang, Y., Guo, L., & Chen, H. (2014). Gear ratio optimization and shift control of 2-speed I-AMT in electric vehicle. *Mechanical Systems and Signal Processing*. https://dx.doi.org/10.1016/j.ymssp.2014.05.045

[20] Sorniotti, A., Subramanyan, S., Turner, A., Cavallino, C., Viotto, F., & Bertolotto, S. (2011). Selection of the Optimal Gearbox Layout for an Electric Vehicle. *SAE International, 4(1),* 1267-1280. doi:10.4251/2011-01-0946